Supporting Information

Exploring the Potential of Lanthanide-Doped Oxyfluoride Materials for Bright Green Upconversion and Their Promising Applications Towards Temperature Sensing and Drug Delivery

*Sonali Mohanty[a,b], Mirijam Lederer[a], Simona Premcheska[a,c], Hannes Rijckaert[d], Klaartje De Buysser[d], Els Bruneel[e], Andre Skirtach[c], Kristof Van Hecke[b], Anna M. Kaczmarek[a]**

Cytotoxicity study

Cell Cultures

Healthy Normal Human Dermal Fibroblasts (NHDFs) were cultured in the appropriate cell growth medium (containing Dulbecco's Modified Eagle Medium (DMEM),10% Fetal Bovine Serum (FBS), 1% Penicilin-Streptomycin) and were seeded in 96-well plates at a concentration of 5,000 cells/well upon reaching optimal confluency state (80-90%) during early culture passage stages (P3-P6). Upon cell seeding the cell plates were incubated in the dark at 37 °C and 5% CO2 for 24 hours before sample addition.

PrestoBlue™ HS cell viability assay

A 2D cell-based assay was performed to preliminarily evaluate the compatibility of the SiO_2@YOF:Yb^{3+},Er^{3+} with in vitro cultured healthy Normal Human Dermal Fibroblasts (NHDFs) by conducting dark cytotoxicity tests. The toxicity evaluation was done utilizing PrestoBlue™ HS reagent in a fluorometric, end-point assay. This resazurin-based cell-permeable reagent, once incubated with metabolically active cells is reduced intracellularly to its highly fluorescent form, resorufin, allowing a very sensitive and directly proportional quantitative assessment of the number of viable cells upon contact incubation with the investigated material. The fluorescence spectroscopy readout was done at λ_{em} = 635 nm, upon excitation at 560 nm.

The toxicity tests were conducted in a concentration-dependent manner in a series of sample concentrations ranging from 0-5 mg/mL where each sample concentration was tested on five technical replicates. The material as dry powder was dispersed in the cell growth medium solution (DMEM: 10% FBS, 1% Pen-Strep) to obtain solution homogeneity and split particle agglomerates by vortexing for 1 minute followed by sonication for 10 minutes. Upon appropriate sample addition, the plates were incubated for 24 hours in the dark at 37 °C and 5% CO_2. After 24 hours long incubation of the cells with the investigated material in varying concentrations, 20 µL of the PrestoBlue™ HS reagent was added to all the wells, and the plates were placed back in dark incubation for 4 hours at 37 °C and 5% CO_2. Both negative and positive controls were included simultaneously: the (sample) negative controls contained seeded cells, cell growth medium, and PrestoBlue™ HS cell viability reagent, while positive controls (or PB-blanks) contained PrestoBlue™ HS cell viability reagent and cell growth medium. The fluorescence emission of the multiwell plates was measured on a Tecan spectrophotometer, equipped with a microplate reader and appropriate optical filters.

The raw data was normalized with respect to the (sample) negative controls, by correcting it to 100% cell viability with the positive controls (and averaging it in the end), in the following way:

$$Cell\ viability\ [\%] = \frac{[FI(technical\ replicate) - FI(positive\ controls\ average)]}{[FI(negative\ control) - FI(positive\ controls\ average)]} \times 100\ (eqn\ 1)$$

Where FI stands for fluorescence emission intensity measured at 635 nm; a technical replicate is a technically repeated sample concentration well containing seeded cells, cell growth medium, sample, and PrestoBlue™ HS cell viability reagent; (sample) negative controls represent plate wells containing seeded cells, cell growth medium solution, and PrestoBlue™ HS cell viability reagent; and positive controls (or PB-blanks) represent plate wells containing cell growth medium and PrestoBlue™ HS cell viability reagent; all equalized to the same final volume per well per plate by cell growth medium solution.

Widefield microscopy imaging

Multiwell plates containing parallel technical replicates were also prepared under identical treatment for widefield microscopy imaging for the same series of sample concentrations, replacing the PrestoBlue™ HS cell viability reagent with Calcein-AM, a

fluorescent cell labeling dye with a concentration of 0.3 µL/well or a final well concentration of 1.5 µM. Upon dye addition, the plates were incubated for 20 minutes in the dark at 37°C and 5% CO_2 to allow dye permeation. The cell visualization was performed on a Nikon-Ti fluorescence microscope equipped with an Andor camera, using a Green Fluorescent Protein (GFP) long-pass filter transmitting all emitted wavelengths ≥ 500 nm, under dye excitation of 470 nm.

Drug loading and drug release study

To study drug loading and release behavior in the hollow YOF:Yb^{3+},Er^{3+} particles, the commonly used water-soluble anti-cancer drug doxorubicin hydrochloride (DOX·HCl) was chosen as the model drug (throughout the manuscript, for simplicity, it will be referred to as DOX). In brief, for each experiment 5 mg of hollow YOF:Yb^{3+},Er^{3+} particles was dispersed in 1 mL phosphate-buffered saline (PBS, pH 7.4) containing 5 mg of DOX. This suspension was left for 24 h at RT with continuous stirring in the dark. Afterwards the particles were centrifuged at 11000 RPM for 10 minutes. The particles were washed and centrifuged repeatedly until a clear supernatant was collected. The supernatant solution was collected for UV-Vis analysis to access the concentration of the DOX which did not load into the particles, using a previously prepared calibration curve (Figure S12). The obtained YOF-DOX was dried overnight in an oven at 80°C. The UV-Vis absorbance was monitored at 480 nm. The amount of DOX loaded into the YOF:Yb^{3+},Er^{3+} was assessed based on the initial mass of DOX and the final mass of DOX detected through UV-Vis absorbance analysis in the supernatant. The drug Loading Capacity (LC%) was calculated using the following formula (eqn 2):

$$LC\% = \frac{mass\ of\ DOX\ in\ YOF}{mass\ of\ DOX\ loaded\ YOF}\ x\ 100\ (eqn\ 2)$$

The drug Encapsulation Efficiency (EE%) was calculated using the following formula (eqn 3):

$$EE\% = \frac{mass\ of\ DOX\ in\ YOF}{mass\ of\ initial\ DOX}\ x\ 100\ (eqn\ 3)$$

The DOX drug release experiments were carried out in PBS buffer at three different pH values: 7.4, 5.5 and 4. In a typical procedure 5 mg of DOX loaded YOF:Yb^{3+},Er^{3+} (DOX-YOF) was dispersed in 0.5 mL PBS buffer. This suspension was poured into a dialysis bag with a cutoff of 6000-8000 Da and tightly secured with clams on both sides. The dialysis bag was placed horizontally in a vial filled with 20 mL PBS buffer. The vial was closed and placed on a shaker (Orbital mini shaker, VWR) set at 37°C. The dialysate containing the released DOX was sampled (3 mL) at appropriate time intervals. The samples were put back to the vial after UV-Vis measurements. The amount of DOX released from the particles was measured by monitoring the absorbance of DOX at 480 nm.

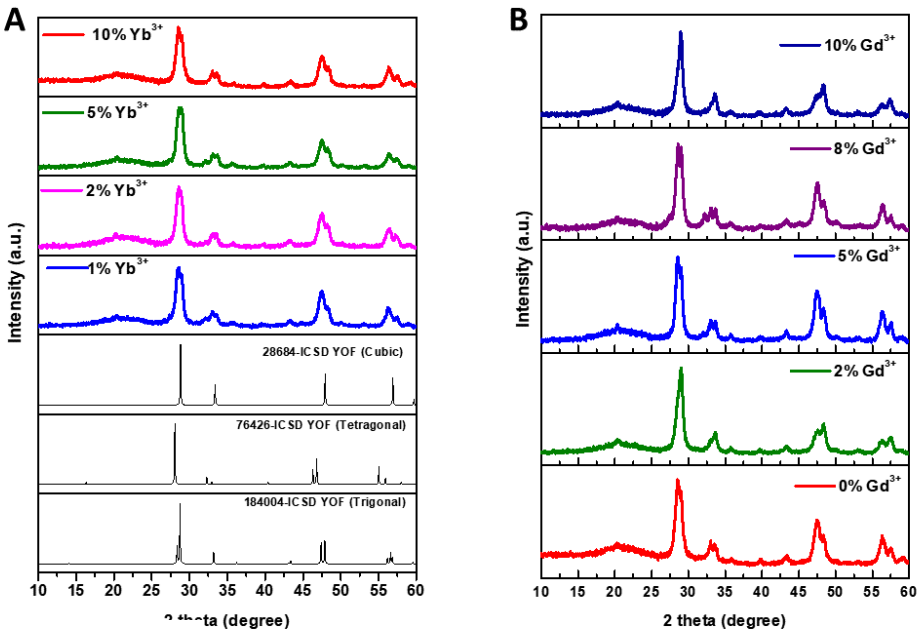

Figure S1. Powder XRD patterns of (A) SiO_2@YOF:x%Yb^{3+},1%Er^{3+} (x = 1%, 2%, 5%, 10%) (B) SiO_2@YOF:10%Yb^{3+},1%Er^{3+},x% Gd^{3+} (x = 2%, 5%, 8%, 10%).

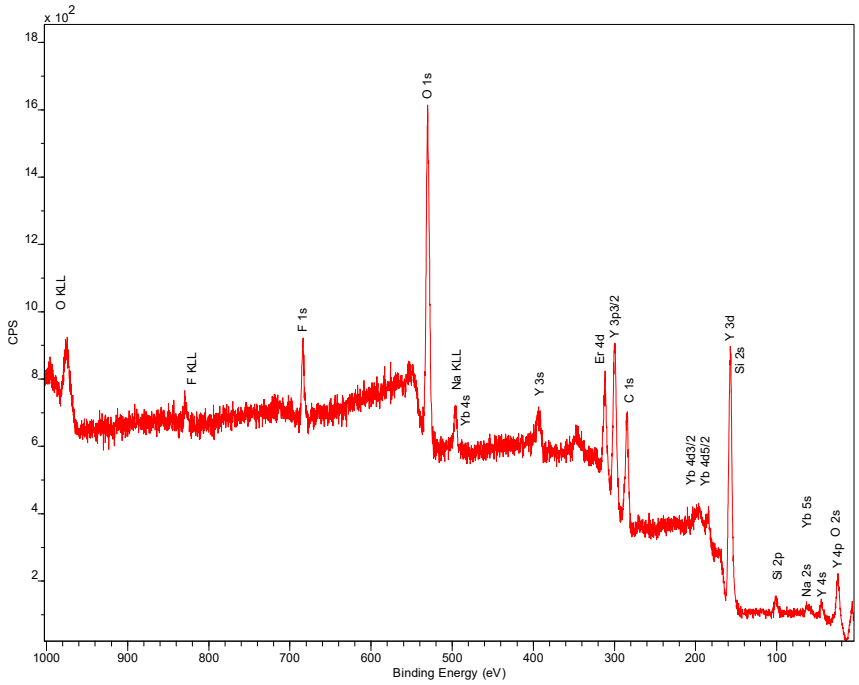

Figure S2. XPS (survey data as well as the simulated Mn2p peaks assuming a Mn/Y ratio of 1/9 in SiO_2@YOF:20%Yb^{3+},1%Er^{3+},10% Mn^{2+}.

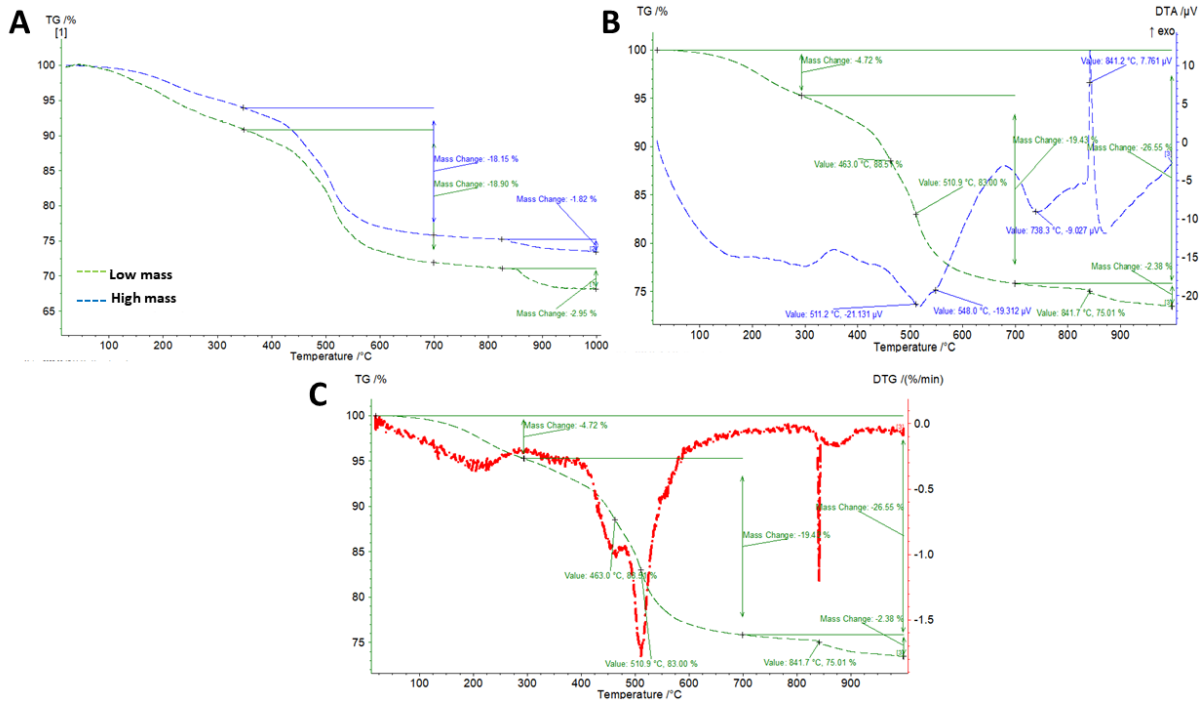

Figure S3. TGA and DTG analysis for SiO_2@$NaYF_4$:Yb^{3+},Er^{3+}.

Table S1: Estimated composition based on XPS analysis for selected samples.

SiO_2@YOF:20%Yb^{3+},1%Er^{3+}, x% Mn^{2+}	O	Y	F	Yb	Mn
10% Mn^{2+}	69.8	16.3	9.9	4.0	0
2% Mn^{2+}	74.7	13.8	8	2.5	0

Table S2: Overview of ICP-OES analysis for all prepared samples.

Compound Name and Theoretical Value (mol %)	mol% Y^{3+}	mol% Yb^{3+}	mol% Er^{3+}	mol% Gd^{3+}	mol% Mn^{2+}	mol% Li^{+}
98%Y^{3+}:**1%**Yb^{3+},**1%** Er^{3+}	97.77	1.20	1.02			
97%Y^{3+}:**2%** Yb^{3+},**1%** Er^{3+}	97.04	2.00	0.95			
94%Y^{3+}:**5%** Yb^{3+} ,**1%** Er^{3+}	94.58	4.38	1.03			
89%Y^{3+}:**10%** Yb^{3+},**1%** Er^{3+}	82.97	16.09	0.94			
79%Y^{3+}:**20%** Yb^{3+},**1%** Er^{3+}	80.82	17.11	2.07			
87%Y^{3+}:**10%** Yb^{3+},**1%** Er^{3+},**2%**Gd^{3+}	86.83	10.08	1.07	2.02		
84%Y^{3+}:**10**% Yb^{3+},**1%**Er^{3+},**5%** Gd^{3+}	83.44	10.49	1.12	4.95		
81%Y^{3+}:**10%** Yb^{3+},**1%**Er^{3+},**8%** Gd^{3+}	80.44	10.36	1.33	7.87		
79%Y^{3+}:**10%** Yb^{3+},**1%**Er^{3+},**10%** Gd^{3+}	77.71	11.19	1.12	9.98		
77%Y^{3+}:**20%** Yb^{3+},**1%**Er^{3+},**2%** Gd^{3+}	70.06	26.60	1.02	2.31		
74%Y^{3+}:**20%** Yb^{3+},**1%**Er^{3+},**5%** Gd^{3+}	71.55	22.00	1.18	5.26		
71%Y^{3+}:**20%** Yb^{3+},**1%**Er^{3+},**8%** Gd^{3+}	68.92	22.28	1.10	7.69		
69%Y^{3+}:**20%** Yb^{3+},**1%**Er^{3+},**10%** Gd^{3+}	58.01	30.65	1.37	9.96		
77%Y^{3+}:**20%** Yb^{3+},**1%**Er^{3+},**2%** Mn^{2+}	77.49	21.22	1.27		0.011*	
74%Y^{3+}:**20%** Yb^{3+},**1%**Er^{3+},**5%** Mn^{2+}	79.48	19.45	1.06		0.074*	
71%Y^{3+}:**20%** Yb^{3+},**1%**Er^{3+},**8%** Mn^{2+}	67.82	30.41	1.77		0.006*	
69%Y^{3+}:**20%** Yb^{3+},**1%**Er^{3+},**10%** Mn^{2+}	71.18	27.36	1.42		0.035*	
77%Y^{3+}:**20%** Yb^{3+},**1%**Er^{3+},**2%** Li^{+}	79.59	18.63	1.78			*
74%Y^{3+}:**20%** Yb^{3+},**1%**Er^{3+},**5%** Li^{+}	79.84	18.38	1.78			*
71%Y^{3+}:**20%** Yb^{3+},**1%**Er^{3+},**8%** Li^{+}	78.48	20.03	1.48			*
69%Y^{3+}:**20%** Yb^{3+},**1%**Er^{3+},**10%** Li^{+}	75.01	23.69	1.29			*

* The identification of these particular metal ions cannot be achieved through the utilization of ICP-OES.

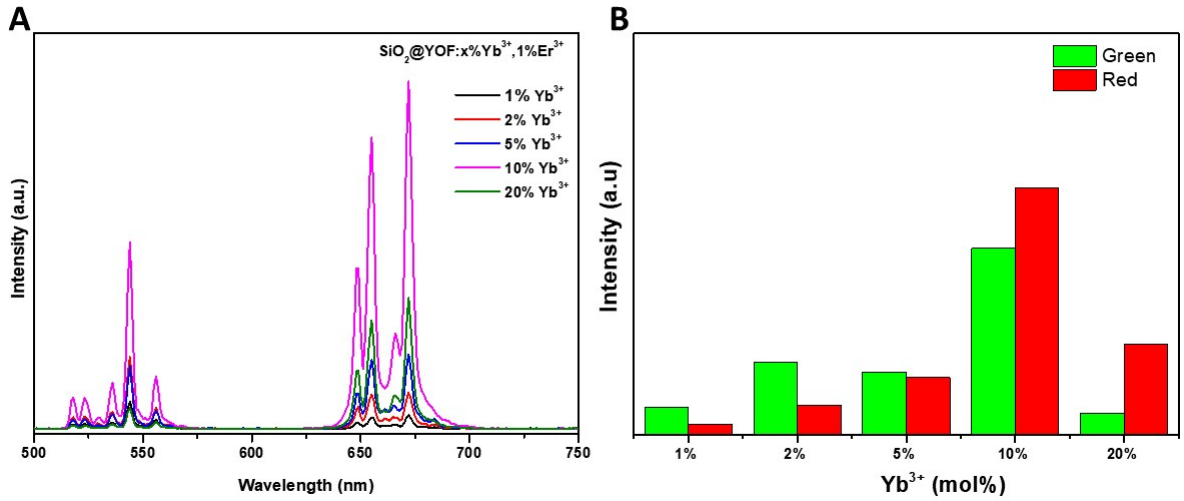

Figure S4. (A) Emission spectra and (B) Green/Red (G/R) ratios for YOF:x%Yb^{3+},1%Er^{3+} where (x = 1%, 2%, 5% ,10%, 20%).

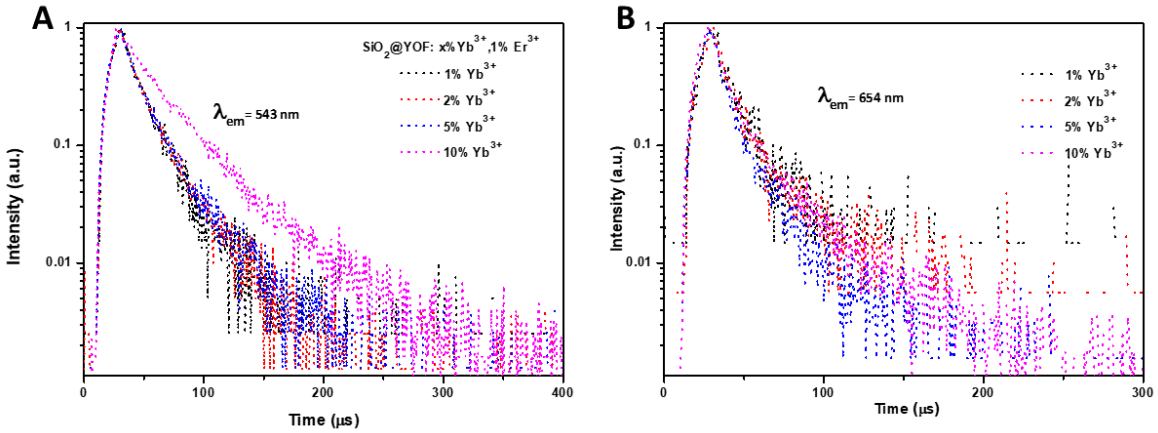

Figure S5. Luminescence decay profiles for (A) green $^4S_{3/2} \rightarrow {}^4I_{15/2}$ (543 nm) and (B) red $^4F_{9/2} \rightarrow {}^4I_{15/2}$ (654 nm) emission peaks in SiO_2@YOF:x%Yb^{3+},Er^{3+} (x = 1%, 2%, 5%, 10%).

Table S3: Overview of decay curves and R^2 of the green $^4S_{3/2} \rightarrow {}^4I_{15/2}$ (543 nm) and red $^4F_{9/2} \rightarrow {}^4I_{15/2}$ (654 nm) emission peaks.

SiO_2@YOF:x%Yb^{3+},1% Er^{3+}	τ_{543} [µs]	R^2
1% Yb^{3+}	118	0.972
2% Yb^{3+}	147	0.991
5% Yb^{3+}	133	0.988
10% Yb^{3+}	264	0.995
20% Yb^{3+}	67	0.990

SiO_2@YOF:x%Yb^{3+},1% Er^{3+}	τ_{654} [µs]	R^2
1% Yb^{3+}	81	0.711*
2% Yb^{3+}	85	0.924*
5% Yb^{3+}	72	0.979
10% Yb^{3+}	103	0.993
20% Yb^{3+}	122	0.997

*The R^2 coefficient of determination for these samples was low, indicating a weak signal, which made it challenging to obtain good-quality decay profiles.

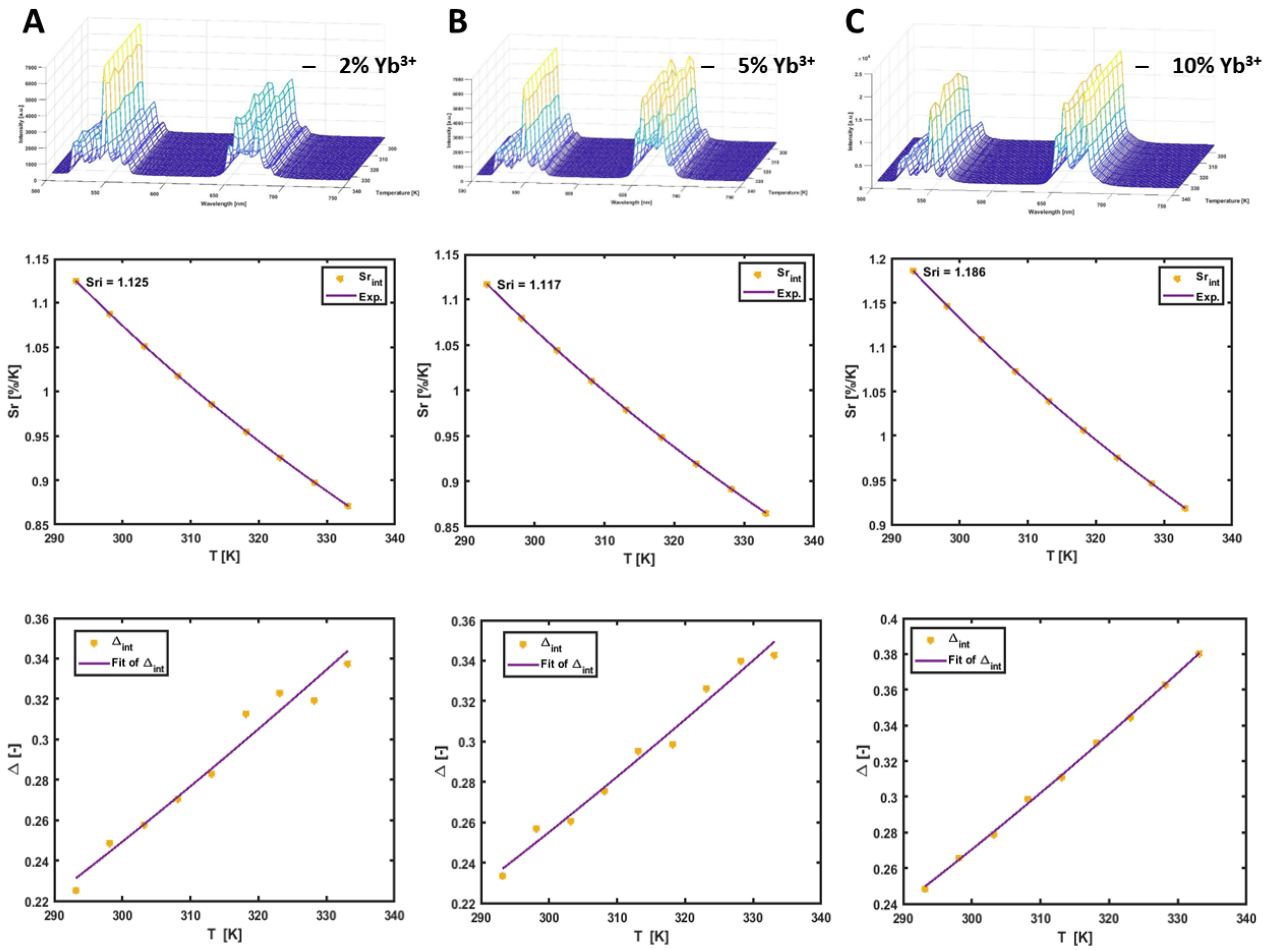

Figure S6. Emission maps, plot of the relative sensitivity (S_r) and the points show the experimental Δ parameters, and the solid line shows the least squares fit to the experimental points varying temperatures: 293.15–333.15 (20–60 °C) for SiO_2@YOF:x%Yb^{3+},1%Er^{3+} (A) 2% Yb^{3+}, (B) 5% Yb^{3+} and (C) 8% Yb^{3+}.

Table S4. Overview of R^2 and S_r values for SiO_2@YOF:x%Yb^{3+},1%Er^{3+}

SiO_2@YOF:x%Yb^{3+},1%Er^{3+}	R^2	S_r (% K^{-1})
2% Yb^{3+}	0.966	1.125
5% Yb^{3+}	0.979	1.117
10% Yb^{3+}	0.998	1.186
20% Yb^{3+}	0.994	0.716

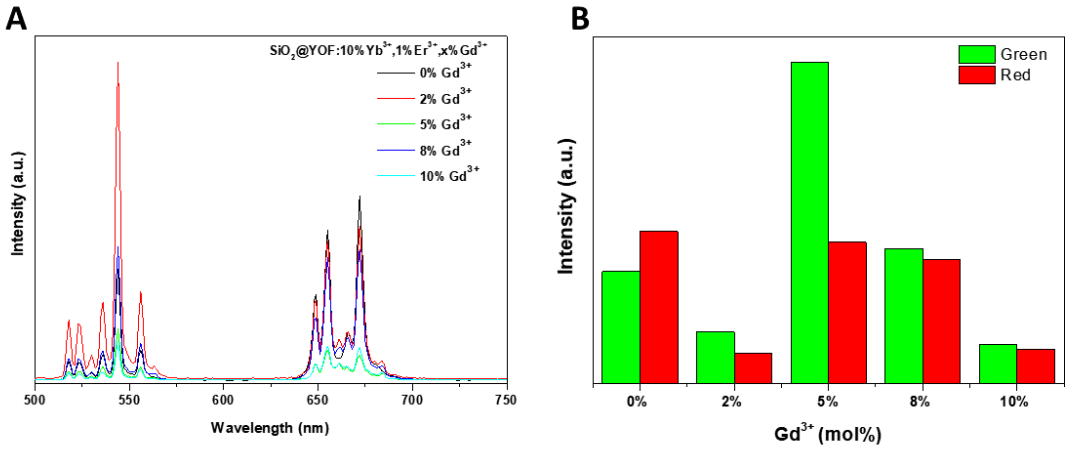

Figure S7. (A) Emission spectra and (B) Green/Red (G/R) ratios for SiO_2@YOF: 10%Yb^{3+},1%Er^{3+},x% Gd^{3+} (x = 2%, 5%, 8%, 10%).

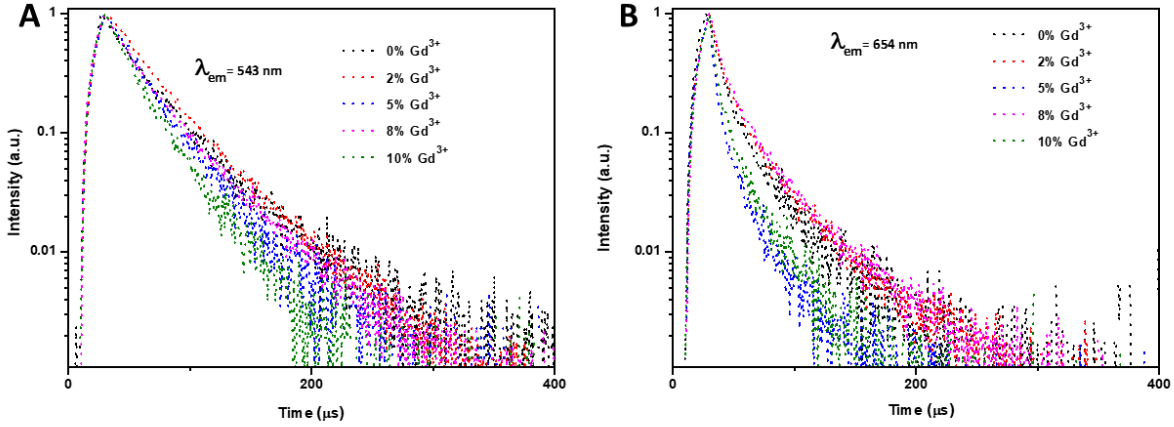

Figure S8. Luminescence decay profiles for (A) green $^4S_{3/2}$→$^4I_{15/2}$ (543 nm) and (B) red $^4F_{9/2}$→$^4I_{15/2}$ (654 nm) emission peaks in SiO_2@YOF:10%Yb^{3+},1%Er^{3+},x% Gd^{3+} (x = 2%, 5%, 8%, 10%).

Table S5. Overview of decay curves and R^2 of the green $^4S_{3/2}\rightarrow{}^4I_{15/2}$ (543 nm) and red $^4F_{9/2}\rightarrow{}^4I_{15/2}$ (654 nm) emission peaks.

SiO_2@YOF:10%Yb^{3+},1%Er^{3+},x% Gd^{3+}	τ_{543} [µs]	R^2
0% Gd^{3+}	264	0.995
2% Gd^{3+}	271	0.991
5% Gd^{3+}	318	0.998
8% Gd^{3+}	240	0.997
10% Gd^{3+}	210	0.990

SiO_2@YOF:10%Yb^{3+},1%Er^{3+},x%Gd^{3+}	τ_{654} [µs]	R^2
0% Gd^{3+}	103	0.993
2% Gd^{3+}	38	0.991
5% Gd^{3+}	86	0.995
8% Gd^{3+}	107	0.996
10% Gd^{3+}	48	0.992

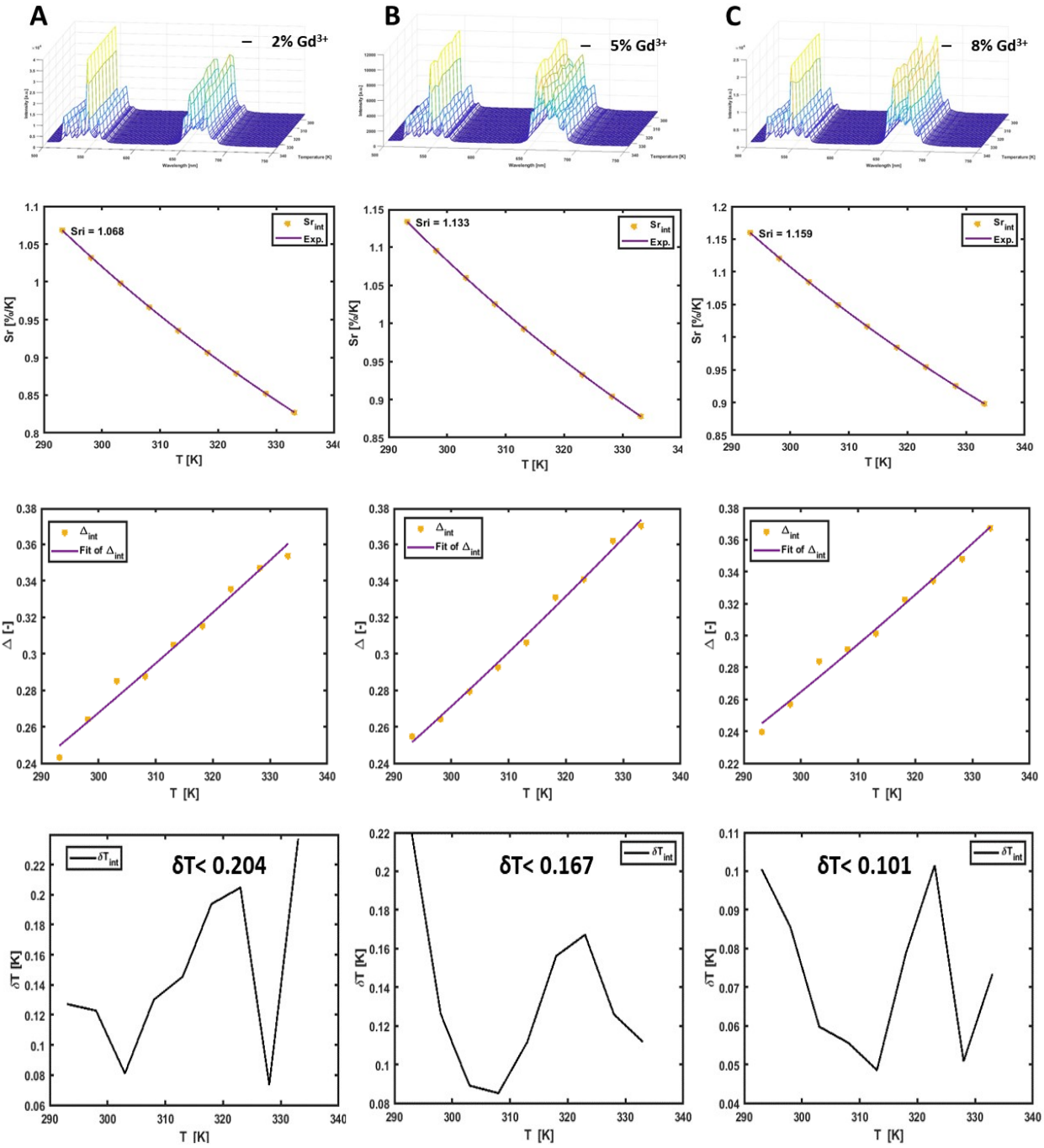

Figure S9. Emission maps, plot of the relative sensitivity (S_r) and the points show the experimental Δ parameters, the solid line shows the least squares fit to the experimental points at varying temperatures: 293.15–333.15 (20–60 °C) and graph depicting the temperature uncertainty in the whole temperature range for SiO_2@YOF:10%Yb^{3+},1%Er^{3+},x% Gd^{3+} where x = (A) 2% Gd^{3+}, (B) 5% Gd^{3+} and (C) 8% Gd^{3+}.

Table S6: Overview of R^2 and S_r values for SiO_2@YOF:10%Yb^{3+},1%Er^{3+},x%Gd^{3+}

SiO_2@YOF:10%Yb^{3+},1%Er^{3+},x%Gd^{3+}	R^2	S_r (% K^{-1})
0% Gd^{3+}	0.998	1.182
2% Gd^{3+}	0.983	1.068
5% Gd^{3+}	0.999	1.133
8% Gd^{3+}	0.988	1.159

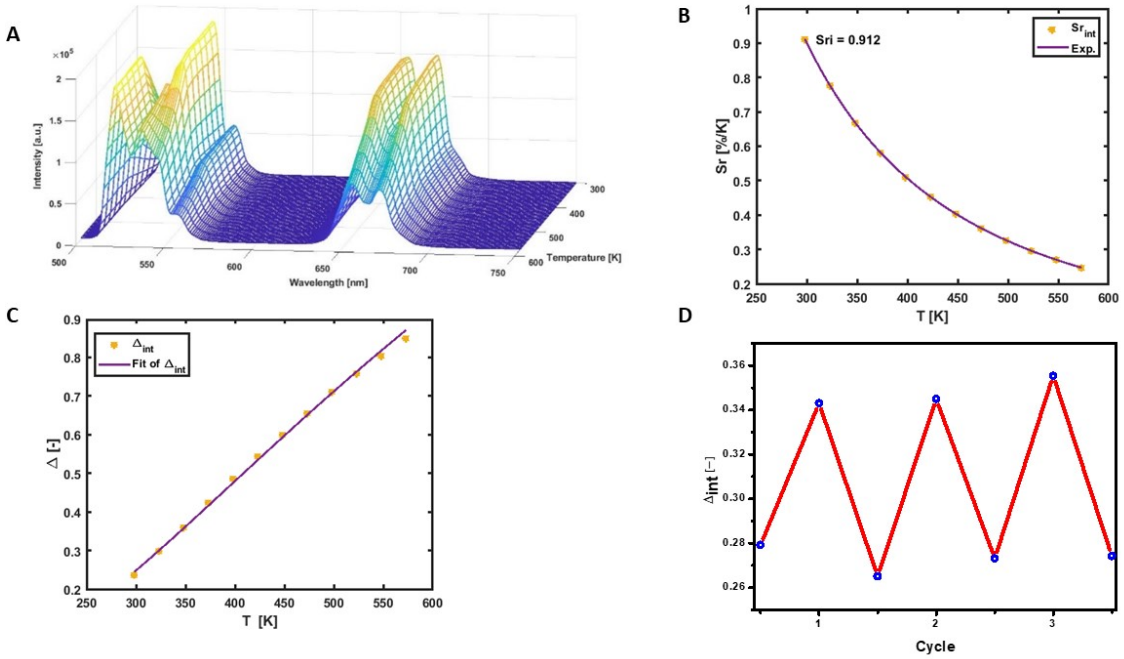

Figure S10. (A) Emission map, (B) S_r sensitivity from 25 to 300 °C (298.15–573.15 K), (C) experimental Δ parameters with the least squares fit for solid SiO_2@YOF:Yb^{3+},Er^{3+},5%Gd^{3+} and (D) cycle test for SiO_2@YOF:Yb^{3+},Er^{3+},5%Gd^{3+} in DI water under two heating–cooling cycles: 293.15 K–333.15 K .

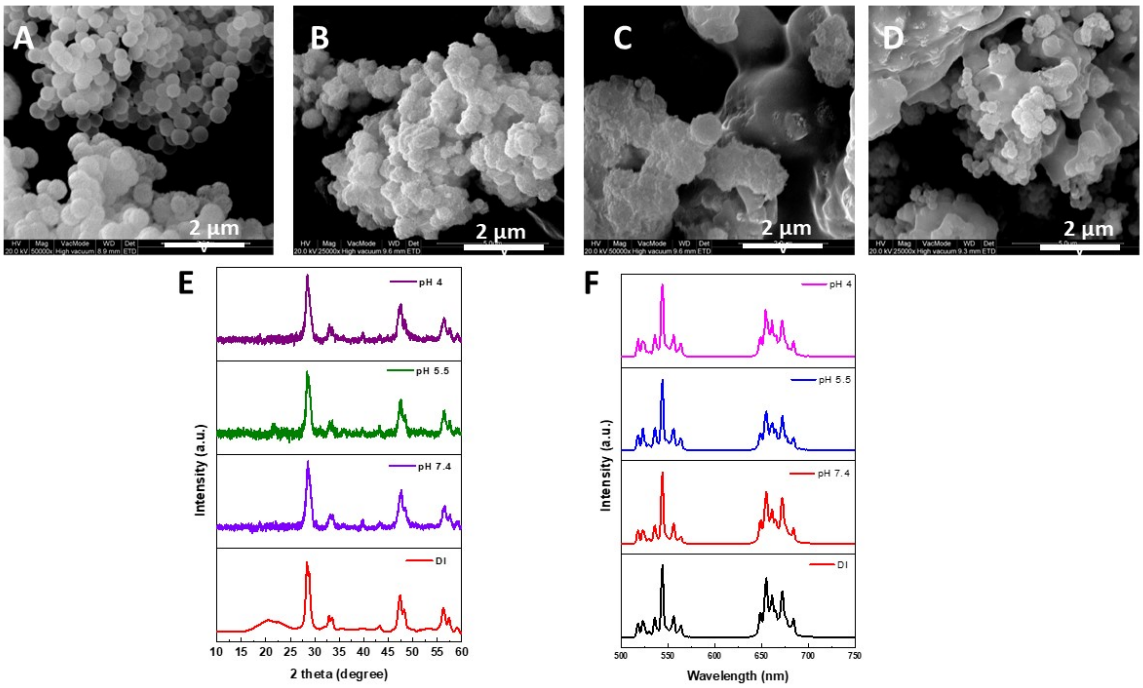

Figure S11. SEM images of (A) pristine SiO_2@YOF:Yb^{3+},Er^{3+},5%Gd^{3+}, and after being immersed in buffer solution for 48 h at varying pH values (B) PBS 7.4, (C) PBS 5.5, (D) PBS 4, (E) Powder XRD patterns of SiO_2@YOF:Yb^{3+},Er^{3+},5%Gd^{3+} after immersing in PBS for 48 h at pH 7.4, pH 5.5 and pH 4 and (F) UC emission spectrum of SiO_2@YOF:Yb^{3+},Er^{3+},5%Gd^{3+} after immersing in PBS with concentration 2mg/ml for 48 h at pH 7.4, pH 5.5 and pH 4.

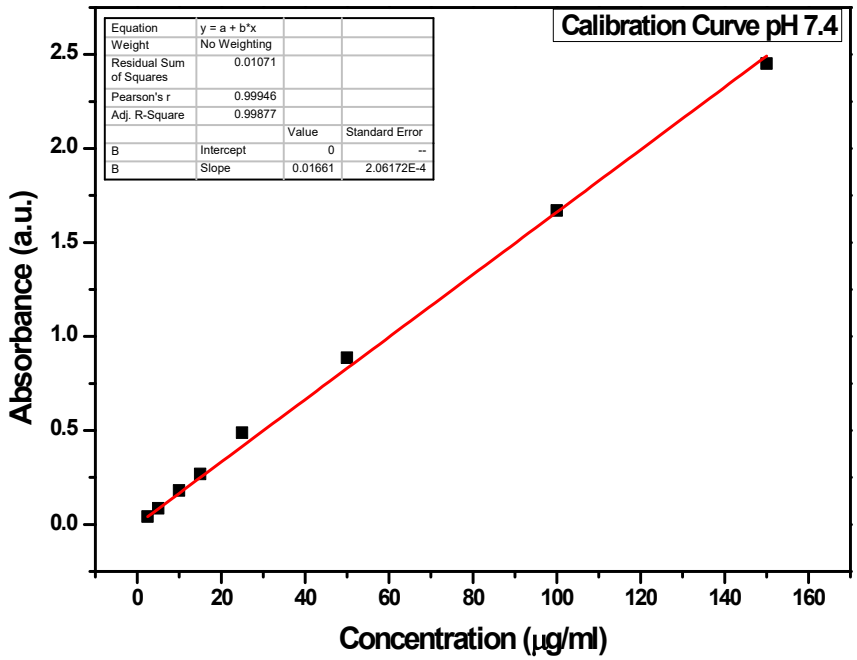

Figure S12. DOX calibration curve for PBS pH 7.4.

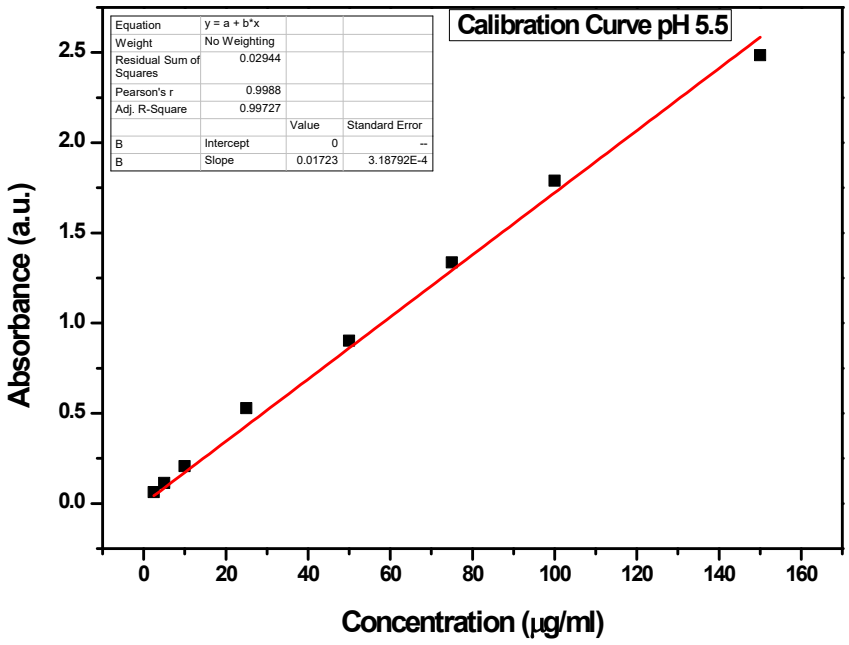

Figure S13. DOX calibration curve for PBS pH 5.5.

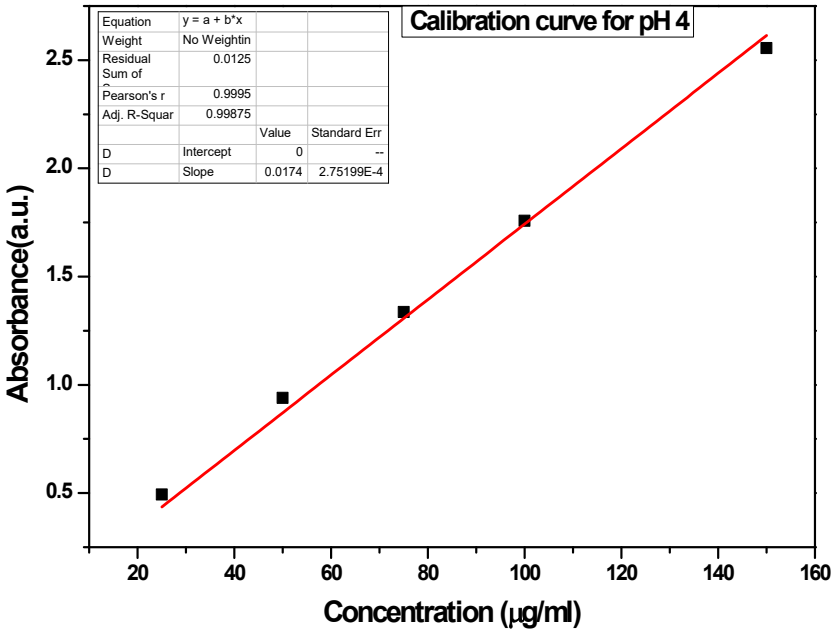

Figure S14. DOX calibration curve for PBS pH 4.

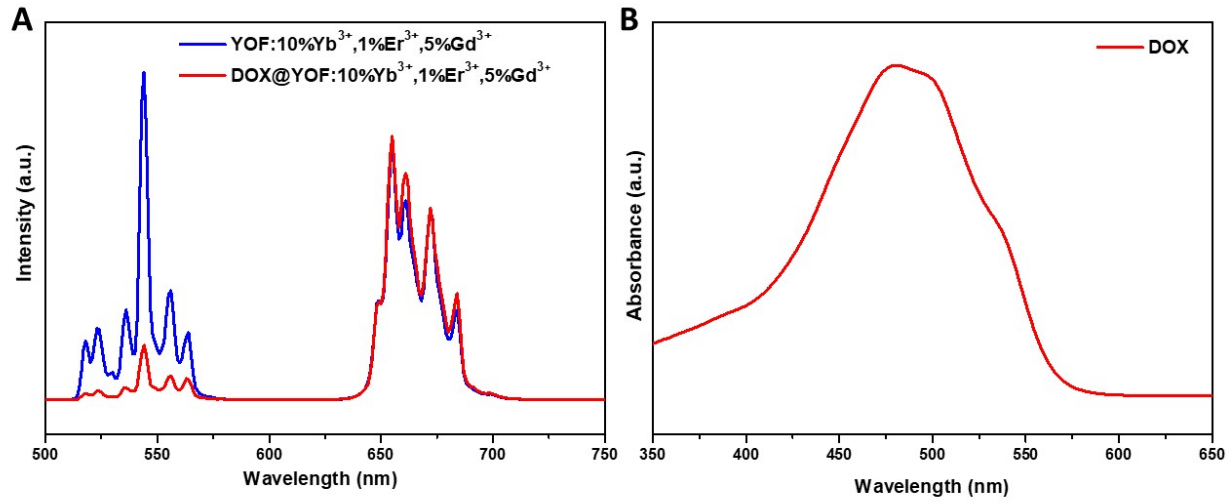

Figure S15. (A) Upconversion emission spectra of YOF:Yb^{3+},Er^{3+},5%Gd^{3+} and DOX@ YOF:Yb^{3+},Er^{3+},5%Gd^{3+} nanocarriers under 975 nm excitation. (B) UV–VIS absorption spectrum of DOX.

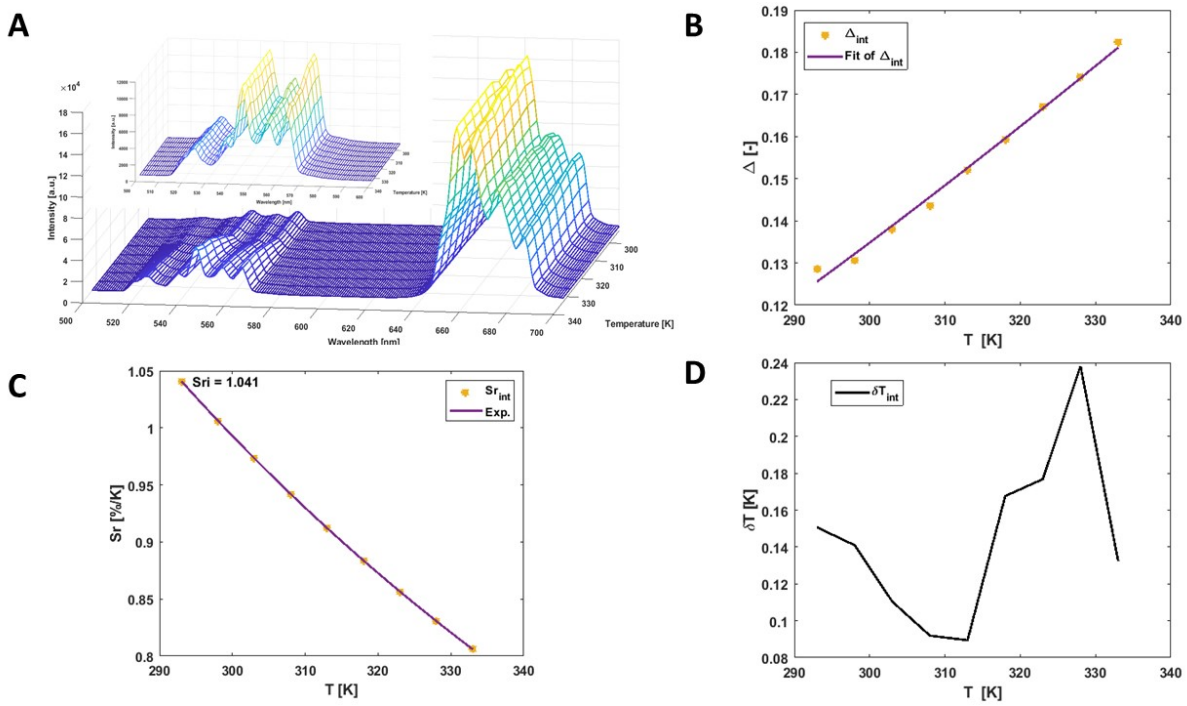

Figure S16. (A) Emission map, (B) experimental Δ parameters with the least squares fit, (C) S_r sensitivity from 20 to 60 °C (293.15–333.15 K) and (D) Graph depicting the temperature uncertainty in the whole temperature range for DOX@YOF:Yb^{3+},Er^{3+},5%Gd^{3+}.

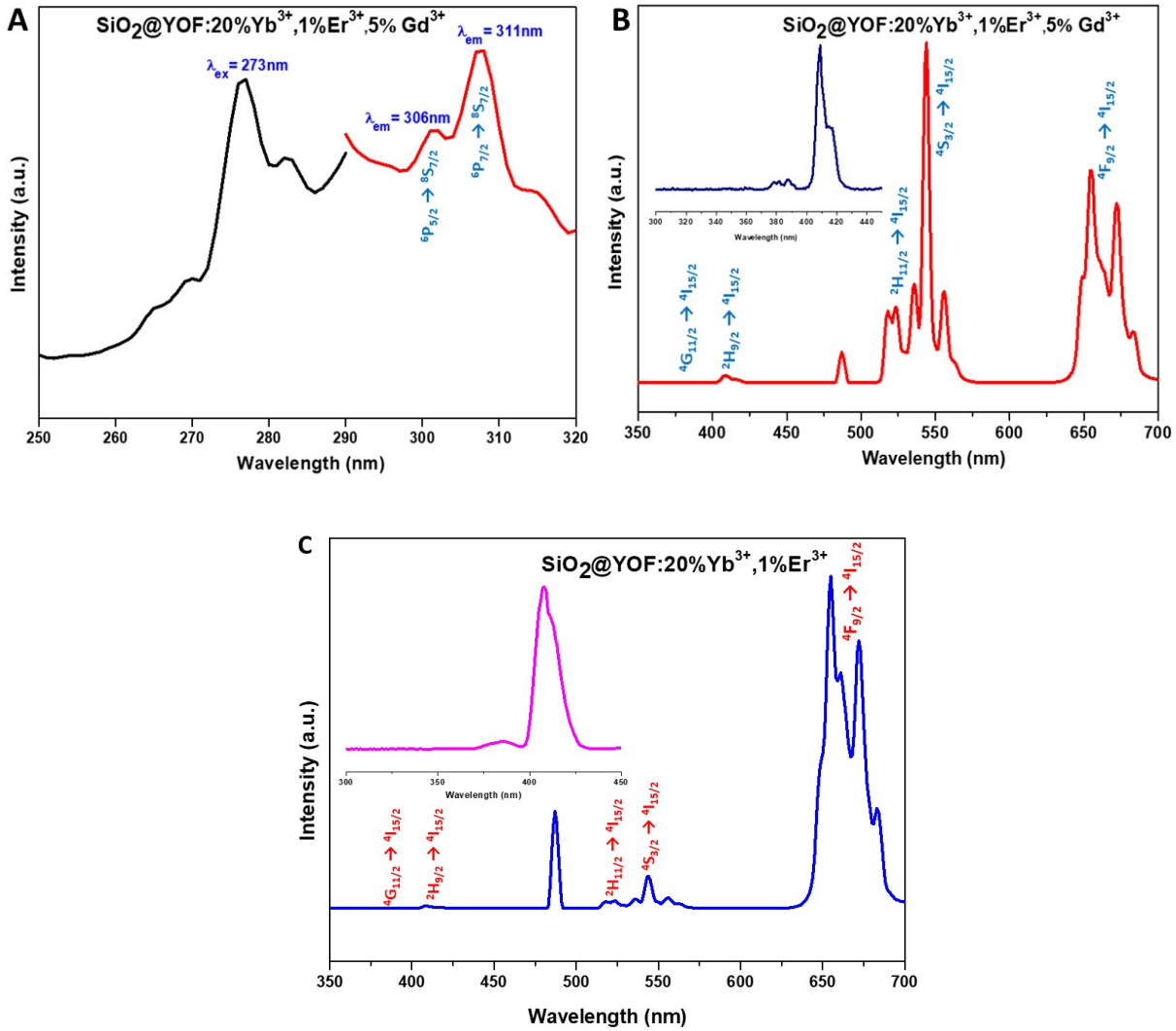

Figure S17. (A) Emission spectra of Gd^{3+} in SiO_2@YOF: Yb^{3+},Er^{3+},5%Gd^{3+} under 273 nm excitation, (B) UC luminescence spectra of SiO_2@YOF:Yb^{3+},Er^{3+},5%Gd^{3+} and (C) SiO_2@YOF:Yb^{3+},Er^{3+} without Gd^{3+}co-doping under 975 nm excitation in the range of 350-700 nm (the sharp peak at 485 nm is likely due to the excitation laser).

.

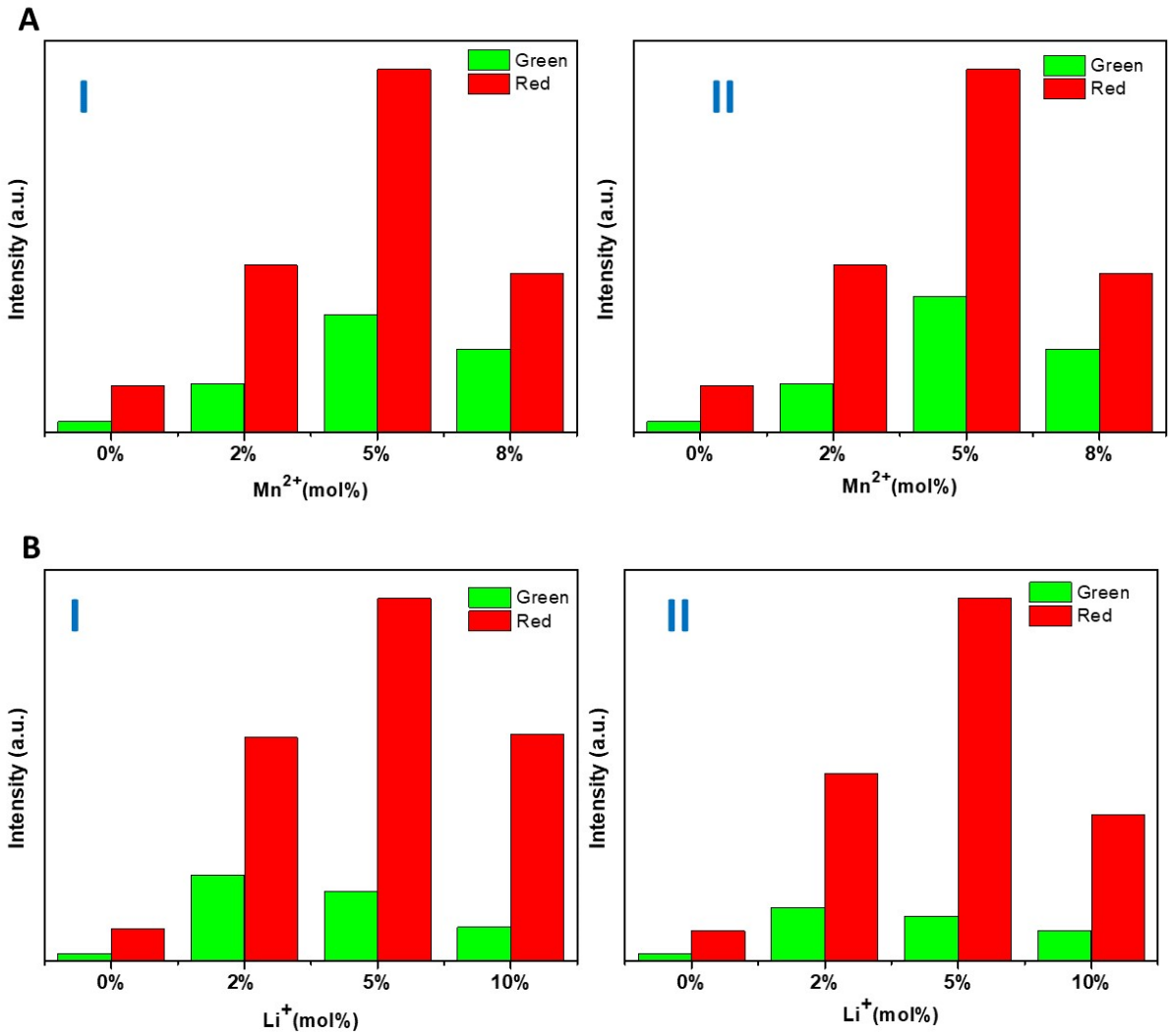

Figure S18. Repeated effect of (A) Mn^{2+} and (B) Li^{+} co-doping concentration on overall G/R intensity in SiO_2@YOF:Yb^{3+},Er^{3+} materials.